Carbon Chemistry of the water column during the GasEx-2001 Experiment

Christopher L. Sabine[1], Richard A. Feely[1], Gregory C. Johnson[1], Peter G. Strutton[2#], Marilyn F. Lamb[1], and Kristene E. McTaggart[1]

[1]Pacific Marine Environmental Laboratory, NOAA
7600 Sand Point Way N.E.
Seattle, Washington 98115-0070 USA

[2]Monterey Bay Aquarium Research Institution
7700 Sandholdt Rd.
Moss Landing, CA 95039-9644

[#]Now at: Marine Sciences Research Center, State University of New York
Stony Brook, NY 11794-5000 USA

Abstract. Three specific studies were conducted as a part of the GasEx-2001 water column program. First, regional surveys were conducted to examine the spatial variability around an array of surface and near-surface drifting instruments. Second, casts were made at noon local time each day to examine the temporal evolution of the water column. Third, two intensive time-series studies were conducted to examine diurnal variations. A mixed layer DIC budget was constructed for the Lagrangian portion of the GasEx study. Over a 13 day period, the net drop in mixed layer DIC was 6.5 μmol kg^{-1}. The net precipitation during this period resulted in a DIC decrease of 1.2 μmol kg^{-1}. Entrainment of DIC from below the mixed layer decreased the net physical effect to 0.9 μmol kg^{-1} (13.5%). Biological new production removed 1.1 μmol kg^{-1} (17.5%) of DIC from the mixed layer. Air-sea gas exchange had the largest impact on the DIC budget, accounting for 69% (4.5 μmol kg^{-1}) of the total DIC removal from the mixed layer during this period. The estimated mean gas transfer velocity for the period that the GasEx array was in the water was 13.8±3.6 cm hr^{-1} (K_{660} = 11.8 cm hr^{-1}). The mean wind speed during this period was 6.0±1.3 m s^{-1}. This gas transfer velocity is in excellent agreement with estimates generated from atmospheric micro-meteorological CO_2 flux measurements collected on the same cruise. The agreement between the oceanic and atmospheric approaches supports the validity of the gas transfer velocities determined for the GasEx-2001 experiment.

1. Introduction

In 1998, NOAA's Office of Global Programs (OGP) initiated a program of process studies to improve quantification of air-sea CO_2 fluxes and gas transfer velocity. The ultimate goal of this effort is to be able to quantify transfer velocities on a regional scale from remote sensing such that, combined with regional sea – air CO_2 partial pressures (ΔpCO_2), improved global air-sea fluxes can be determined. To accomplish this goal, fluxes have to be determined at the same (hourly) time scale as the variability in environmental forcing. The first gas exchange experiment, GASEX-98, occurred in the CO_2 sink region of an anticyclonic warm core ring in the eastern North Atlantic during May and June of 1998 [*Wanninkhof and McGillis*, 1999; *McGillis et al.*, 2001a; *McGillis et al.,* 2001b; *Feely et al.*, 2002]. Air-sea gas exchange was studied using a variety of direct and indirect approaches.

The GasEx-2001 study took place aboard the NOAA Ship *RONALD H. BROWN* in the eastern Equatorial Pacific in February and March, 2001. The low annual mean wind speeds in the Equatorial Pacific and high ΔpCO_2 values, offered a unique opportunity to directly determine the fluxes in a low wind stress environment and to elucidate the factors controlling the flux. Most of the GasEx-2001 experiments involved measurements taken by and around a drifting array of near-surface instruments deployed at 3.00°S, 125.00°W on 23:35 UTC February 14, 2001. The GasEx array was allowed to drift for approximately 14 days until 08:00 UTC March 1, 2001. Over this time period, the array drifted approximately 731 km to 2.30°S, 131.54°W.

Three specific studies were conducted as a part of the GasEx-2001 water column program (Figure 1). First, regional surveys of the study area were conducted at the beginning and middle of the study period to examine the spatial variability around the array. Second, casts were made near the GasEx array at noon local time (20:00 UTC) each day to examine the temporal evolution of the water column hydrography and carbon distributions over the course of the experiment. Third, two intensive time-series studies were conducted with casts every three hours to examine diurnal variations in the water column. These studies were used to characterize the spatial and temporal evolution of the ocean system over the course of the experiment. The large-scale physical oceanographic setting and temporal evolution of the hydrographic conditions are described elsewhere [*Johnson et al.*, 2003; *Johnson and Sabine*, 2003]. This work examines the inorganic carbon budget over the course of this experiment in an attempt to isolate the gas exchange component of the budget.

1.1 DIC Budget

Changes in mixed layer dissolved inorganic carbon (DIC) concentrations are a function of: air-sea gas exchange; biological uptake/respiration; and horizontal and vertical mixing processes. *Chipman et al.* [1993] studied DIC distributions in a warm core eddy from the North Atlantic in 1990 and found that biological utilization of carbon and air-sea gas exchange were the predominant processes controlling CO_2 distributions in the mixed layer. Horizontal mixing and vertical entrainment of DIC from depth into the mixed layer were negligibly small. A DIC budget was also constructed for the GasEx-98 study in a similar North Atlantic eddy [*Feely et al*., 2002]. The *Feely et al.* study found that approximately 43% of the total change in DIC was due to entrainment, 30% was due to biological uptake and carbon export flux, and the remaining 27% was due to air-sea exchange of CO_2 (i.e. 0.84 μmol kg^{-1} d^{-1}). Using the GasEx-98 DIC budget for the three-day period from June 16-19, 1998, *Feely et al.* estimated a gas exchange velocity of 19 ± 11 cm/hr for an average wind speed (U_{10}) of 9 m s^{-1}. This estimate was consistent with estimates based on the atmospheric eddy correlation studies of *Wanninkhof and McGillis* [1999] and *McGillis et al*. [2001a] on the same cruise.

The GasEx-2001 study used the same basic approaches to evaluate the DIC budget and gas exchange velocity in an area with relatively low wind speeds and large positive ΔpCO_2 values. Although this study attempts to isolate a relatively small signal from the large overall variability, it provides an independent check on the direct flux measurements. It also provides the only means available for estimating the CO_2 gas flux for the GasEx-2001 experiment directly from seawater measurements. All of the other gas exchange techniques used for this study were based on atmospheric measurements. Consistency between the micro-meteorological CO_2 measurements in the atmosphere and the CO_2 loss from the water column suggest that there are not any major unknown biases in the various approaches.

2. Data

Forty-one casts were conducted in the main study area using a Seabird CTD 911plus/ rosette system (Figure 1). All casts were made within a few kilometers of the GasEx array except when the regional surveys were being conducted. Continuous profiles of temperature, salinity, pressure, and oxygen were collected with estimated accuracies of 0.002°C, 0.003 PSS-78, 2 dbar,

and 2 μmol kg^{-1}, respectively. Water samples were collected from 23 Niskin bottles closed at 17 nominal pressures in the upper 500 m of the water column.

DIC measurements were made using a single operator multiparameter metabolic analyzer (SOMMA)-coulometer system based on the principles outlined by *Johnson et al.* [1985; 1987]. The precision and accuracy of the SOMMA TCO_2 system is estimated to be about ±1.5 μmol kg^{-1} based on the analysis of duplicate samples and certified reference materials (CRMs) prepared by A. Dickson of Scripps Institution of Oceanography [*Dickson*, 2003; *Dickson et al.*, 2003].

Discrete pCO_2 measurements were made on 500 ml samples using a non-dispersive infrared analyzer (NDIR) following the techniques of *Wanninkhof and Thoning* [1993] and *Chen et al.* [1995]. All samples were equilibrated to a temperature of 20°C before analysis. The precision and accuracy of the pCO_2@20°C measurements in the mixed layer is estimated to be about ±0.64 μatm based on the analysis of 44 duplicate samples.

Nutrient measurements were made by autoanalyzer using the associated chemistry and standardization procedures designed and utilized on the WOCE and JGOFS programs [*Gordon et al.*, 1993]. Accuracy is estimated to be approximately 1% of full range, or 0.4 μmol kg^{-1} for nitrate (NO_3) and 0.03 μmol kg^{-1} for phosphate (PO_4).

Samples were also collected and analyzed for chlorophyll (usually 11 depths from 0 to 200m at every station), productivity (^{14}C uptake from 7 depths between 0 and ~120m at almost every station), and new production ($^{15}NO_3$ and $^{14}NH_4$ uptake from 6 depths between 0 and ~80m at one station per day). The details of the biological measurements, including techniques and results, are given in *Strutton et al.* [2003].

3. Spatial Distribution of Carbon

The distributions of water properties during the GasEx-2001 experiment were typical of the eastern Equatorial Pacific during weak La Niña conditions. To characterize the near-field distribution of properties at the beginning of the GasEx-2001 experiment, a series of hydrocasts were conducted in a butterfly pattern centered on the location (3°S, 125°W) where the drifting array would be deployed (Figure 1). Sections of temperature (T), salinity (S), DIC, and pCO2@20°C along the meridonal axis of the butterfly are shown in Figure 2. The strong tropical thermocline that separates the warm near-surface layer (T>25°C) from the equatorial 13°C

thermostad shoals toward the equator (Figure 2a). Surface waters were generally colder closer to the equatorial upwelling and warmer to the south.

The salinity section shows more structure than temperature, reflecting the large scale circulation and water flux patterns of the Equatorial Pacific (Figure 2b). The north end of the section shows the low salinity equatorial surface waters with higher salinity waters to the south. High salinity subsurface water also approaches the equator from the south while relatively fresh waters move south, reflecting the mean geostrophic convergence that feeds the Equatorial Undercurrent and supplies the equatorial upwelling [*Tsuchiya*, 1968; *Johnson and McPhaden*, 1999].

The pCO_2 of seawater is strongly affected by changes in temperature. Examination of the pCO_2 of the waters normalized to a constant temperature shows the changes in carbon chemistry along the section that are independent of the temperature forcing (Figure 2c). Without the temperature effect, the pCO_2 distribution shows a sharp increase within the thermocline and a shoaling of the isopleths toward the equator. This rapid increase in pCO_2 with depth primarily results from the decomposition of organic matter in the water column [*Volk and Hoffert*, 1985]. Biological productivity in the surface waters, and hence DIC uptake, in the Equatorial Pacific is limited by iron availability [*Chavez and Barber*, 1987; *Coal et al.*, 1996]. Most of the thermocline high CO_2 signal reflects organic matter decomposition that has occurred at higher latitudes and was advected towards the Equator [*Chavez and Barber*, 1987].

The thermodynamic response of seawater pCO_2 to a one degree change in temperature is approximately 4.23% [*Takahashi et al.,* 1993]. The decrease in thermocline temperatures with depth lowers the in situ pCO_2 by nearly 300 µatm at 200 m, thus generating a much weaker vertical gradient in the in situ pCO_2. Correcting the pCO_2 values to in situ conditions also increases the warm surface pCO_2 values by nearly 100 µatm, making the surface waters supersaturated with respect to the atmosphere. This supersaturation reflects the excess carbon that is stored in the recently upwelled waters. As the new surface waters warm, the pCO_2 increases, strengthening the thermodynamic drive for CO_2 to evade into the atmosphere. Although biological production and air-sea gas exchange work to decrease the surface pCO_2 concentrations, warming of the waters over time counteracts this to maintain the high seawater CO_2 concentrations. Variations in near-surface pCO_2 are discussed in detail in other papers [*DeGrandpre et al*., 2003; *Wanninkhof et al.*, 2003].

Like pCO_2, DIC is strongly affected by the biological pump [*Volk and Hoffert*, 1985]. As with the pCO_2@20°C, there is a rapid increase in DIC concentrations with depth in the thermocline (Figure 2d). However, some of the physical forcing, as evidenced by the structure in the salinity section (e.g. the low surface salinity at the north end of the section), is more prevalent in DIC than in pCO_2. DIC is a state variable, thus it is not affected by changes in temperature and only reflects true changes in the mass balance. DIC exhibits a relatively strong increase in surface concentrations towards the south, from a mean value of 2029 μmol kg^{-1} in the upper 30m at 2.25°S to 2046 μmol kg^{-1} at 3.75°S. This increase likely reflects both water-mass changes and meridional gradients in biological productivity.

The zonal changes in all four parameters are much smaller than the meridional changes over the same distances (Figure 3). However, there was a consistent decrease in all parameters toward the west. Zonal changes in mean surface layer DIC, for example, dropped from 2042 μmol kg^{-1} at 124.25°W to 2037 μmol kg^{-1} at 125.75°W. Similar meridional and zonal gradients were observed in the second butterfly survey conducted near the midpoint of the study period.

4. Temporal Evolution of DIC

The main portion of the GasEx-2001 study centered on a floating array of instruments that were outfitted with a drogue to remain with the same water mass as a Lagrangian type study. Daily hydrocasts were collected within a few kilometers of the array to characterize the evolution of the water mass properties over the course of the experiment. By constructing a DIC budget for the surface waters, the temporal evolution of the DIC concentrations can be used to estimate the carbon lost from the ocean due to gas exchange during this study.

Within the mixed layer, the daily changes in DIC can be expressed as the sum of changes in DIC due to evaporation and precipitation (ΔDIC_{EP}), vertical mixing (ΔDIC_{mix}), production/decomposition of dissolved organic carbon (ΔDIC_{DOC}), production/decomposition of particulate organic carbon (ΔDIC_{POC}), production/remineralization of particulate inorganic carbon (ΔDIC_{PIC}), and air-sea gas exchange (ΔDIC_{exch}):

$$\Delta DIC_{total} = \Delta DIC_{EP} + \Delta DIC_{mix} + \Delta DIC_{DOC} + \Delta DIC_{POC} + \Delta DIC_{PIC} + \Delta DIC_{exch} \qquad (1).$$

Thus, one can quantify the effect of gas exchange on the DIC budget by correcting the observed total change in DIC for the physical ($\Delta DIC_{EP} + \Delta DIC_{mix}$) and biological ($\Delta DIC_{DOC} + \Delta DIC_{POC} + \Delta DIC_{PIC}$) effects:

$$\Delta DIC_{exch} = \Delta DIC_{total} - (\Delta DIC_{EP} + \Delta DIC_{mix})_{physical} - (\Delta DIC_{DOC} + \Delta DIC_{POC} + \Delta DIC_{PIC})_{biological} \quad (2).$$

In the following sections we will examine the individual components of this relationship.

4.1 Total Changes in DIC

Since air-sea gas exchange is limited to the waters in direct contact with the surface, this work focuses on variations within the mixed layer. Low wind-driven turbulence and large diurnal variations in latent and sensible heat fluxes can result in significant stratification during the daylight hours that is quickly mixed out at night [*Ward et al.*, 2003]. Although this stratification can impact the short-term (minutes to hours) carbon cycle and fluxes [*Wanninkhof et al.*, 2003], a water mass definition that considers the larger scale mixing that occurs over the diurnal cycle is more appropriate for the longer term (days to weeks) DIC budget calculations. Unfortunately, the standard definitions of mixed layer depth (e.g. changes in temperature, salinity or density relative to the surface, or depths where the vertical gradients of these quantities exceed some values) did not work well for our purposes with the entirety of measurments made during GasEx-2001.

For this work, the mixed layer is considered to be all waters with a potential density (σ_θ) less than 23.1 kg m^{-3}. This criterion was based on several observations. First, mixed layer estimates based on ΔT or ΔS definitions for nighttime casts collected as part of the two intensive studies indicated that mixed layer depths were comparable to the depth of σ_θ = 23.1 kg m^{-3}. Second, a section of potential density as a function of time shows that the 23.1 kg m^{-3} surface was one of the lowest density surfaces present throughout the experiment (Figure 4). Finally, a plot of several physical and biogeochemical properties as a function of potential density show relatively consistent concentrations at densities less than 23.1 kg m^{-3}, and increasing scatter at higher densities (Figure 5).

The average mixed layer depth determined for this study was 42±6 m. The temporal change in DIC concentration was determined by averaging the sample values, typically 7-9

bottles, collected in the mixed layer from the daily noon casts conducted near the array. Although the intensive studies at the beginning and middle of the experiment indicate that there was a diurnal cycle of approximately 1.5 μmol kg^{-1} in DIC, the potential bias from a once-per-day sampling approach should be minimized by the fact that the daily casts were always collected as close to local noon (20:00 UTC) as possible. The diurnal DIC cycle primarily reflects the light-dark response of the biological production, with local noon marking the minimum daily DIC concentrations for both intensive study periods.

The total change in mixed layer DIC over the 13 days of the experiment was a lowering from 2038 μmol kg^{-1}, when the array was first deployed, to 2031.5 μmol kg^{-1} when the array was recovered at the end of the experiment. As noted in equation (1), this drop of 6.5 μmol kg^{-1} represents the cumulative effects of both the physical and biological controls on DIC (Figure 6).

4.2 DIC Changes Due to Physical Factors

The two dominant physical fluxes that must be considered in a Lagrangian mixed layer DIC budget are surface exchanges and vertical mixing and diffusion from below. Since DIC concentrations increase rapidly with depth below the mixed layer, vertical entrainment could have a significant impact on the average mixed layer concentrations. The GasEx-2001 site, however, has a relatively low energy environment with weak winds and a strong tropical thermocline. The observed mixed layer depths were very stable over the course of the experiment, suggesting that vertical mixing was relatively small. To quantify the potential vertical DIC fluxes, a simple one-dimensional mixed-layer model (PWP) was run. The model domain extended from the surface to 500 m at one meter intervals and was initialized with temperature, salinity, and DIC profiles from a hydrocast conducted just prior to deployment of the GasEx array. The model was forced with observed meteorological conditions and is described in detail by *Johnson and Sabine* [2003]. Background vertical diffusivity used in the model ($K_z = 1x10^{-6}$ m^2 s^{-1}) is at the lower end of the observed range of thermocline values [*Gregg*, 1998]. Upwelling is prescribed in the model at a rate of $1x10^{-5}$ m s^{-1} based on the observed thermocline shoaling of 13 m over the 15.5 days of that the ship was in the study region. Observed and modeled temperature profiles at the end of the experiment are in very good agreement, with temperature differences above the thermocline of only 0.05°C. Treating DIC as a passive tracer that is affected by physical mixing, but not biology, the model predicts an

increase in mixed layer DIC of 0.4 μmol kg^{-1} over 15.5 days. While all of the DIC increase is ostensibly attributed to entrainment at the base of the mixed layer, this entrainment is about 25% lower in a model run without prescribed upwelling.

Air-sea fluxes have a much stronger influence on the mixed layer DIC concentrations than the physical fluxes from below. Since the air-sea exchange of DIC is the objective of this study, that component will be examined later. Another surface flux that must be considered is the air-sea exchange of water. Precipitation and evaporation dilute or concentrate DIC in the same ratio as salinity. To remove this effect from the total DIC signal, the mixed layer DIC values were normalized to the salinity from the first hydrocast of the experiment. The first 6 days of the experiment showed a small net decrease (~0.1%) in observed mixed layer salinity. After day 52.8, salinity increased to reduce to overall drop in salinity to ~0.04% for the experiment. This equates to approximately 0.8 μmol kg^{-1} decrease in DIC due to dilution.

Although the PWP model included observed meteorological forcing using shipboard estimates of precipitation and evaporation, it did not adequately reproduce the net lowering of salinity observed during the first half of the experiment. This deficiency most likely resulted from the fact that the rain during the first few days of the experiment was generally confined to isolated squalls which may not have passed directly over the ship where the rainfall was recorded. The latter half of the experiment there were fewer rain squalls and the modeled changes in salinity resulting from a net evaporation agree very closely with the observations.

The net effects of the physical fluxes on the mixed layer DIC can be seen in Figure 6. The DIC_{phys} values show the DIC values after being corrected for the physical fluxes. Most of the separation between the DIC and the DIC_{phys} trends prior to day 52.8 result from a net freshening of the mixed layer. After day 52.8 the net evaporation in the mixed layer decreased the DIC dillution by about half. Removing the effects of the physical fluxes reduces the net drop in DIC over the 13 days of the experiment from 6.5 to 5.7 μmol kg^{-1}.

4.3 DIC Changes Due to Biology

Biological production and decomposition can affect DIC concentrations in several ways. One direct affect on DIC is the precipitation of particulate inorganic carbon (PIC). The production of calcitic (e.g., coccoliths and forams) and aragonitic (e.g., pteropods) plankton tests

not only decreases the DIC, but also decreases the total alkalinity (TA) in a ratio of TA:DIC = 2:1 according to:

$$2HCO_3^- + Ca^{2+} = CO_2 + CaCO_3 + H_2O \quad (3)$$

Since TA is a sensitive indicator of carbonate production and is not strongly affected by the biological production of organic matter, the ΔDIC_{PIC} term in the DIC budget can be estimated from TA changes during the experiment. Although there is some variability in the TA calculated from DIC and pCO_2, there is no clear trend over the time frame of the experiment (Figure 7). Even when normalized to a constant salinity, the slope of a linear fit is not significantly different from zero (0.1±1.0 μmol kg^{-1} d^{-1}). Thus, ΔDIC_{PIC} is taken to be zero for these budget calculations.

There is also no observable trend in the dissolved organic carbon (DOC) concentrations during the experiment (Figure 7). Significant conversions of DIC to the dissolved organic pool or the decomposition of DOC back to DIC could impact the DIC budget, but the ΔDIC_{DOC} appears to be zero within the precision of the measurements.

The largest impact of biology on the DIC budget is the production and export of particulate organic carbon (ΔDIC_{POC}). The observed production based on ^{14}C incubations (average = 0.83±0.23 mmol m^{-3} d^{-1}) was very large compared to the net changes observed in DIC. However, much of that production is quickly recycled within the mixed layer. The details of the productivity measurements and the temporal changes in biological production are given by *Strutton et al.* [2003]. New production estimates were evaluated on 13 casts during this experiment using ^{15}N enrichment experiments. A mean profile of the *f* ratio (the ratio of new production to ^{14}C production) based on these experiments showed a decrease from 0.165 at the surface down to 0.04 at 60 m. The net result was roughly equivalent to a new production of about 10% within the mixed layer. The $DIC_{phys\&Cbio}$ points on Figure 6 were determined by correcting the DIC_{phys} for new production by applying the observed *f* ratio profile to the daily ^{14}C production estimates in the mixed layer. The net change in DIC after removing the physical and biological fluxes during the experiment was a decrease of 4.5 μmol kg^{-1}.

An alternative approach for estimating new production in the mixed layer is to examine the net change in inorganic nutrients over time. As a validation for the new production estimates

given above, the changes in inorganic nitrogen were examined. First, the nitrate plus nitrite values were normalized to a constant salinity in the same way as the DIC samples. To convert the nitrogen to carbon, the daily change in salinity normalized total dissolved inorganic nitrogen (ΔN) was multiplied by a C:N of 7.31 estimated by *Anderson and Sarmiento* [1994]. Figure 6 shows the $DIC_{phys\&Nbio}$ points determined by correcting the DIC_{phys} for the nitrogen based biological production estimates. Although there is significant variability in the first half of the experiment, the net changes agree very well with the productivity based estimates.

4.4 DIC Changes Due to Gas Exchange

Based on the mass balance in equation (2), the change in $DIC_{phys\&Cbio}$ over time reflects the loss of CO_2 from the mixed layer due to air-sea gas exchange. To determine the average mixed layer DIC loss due to gas exchange, the $DIC_{phys\&Cbio}$ data were fit as a linear function of time. The resulting slope was -0.254±0.055 μmol kg^{-1} d^{-1}. Over this 13 day period, the net drop in mixed layer DIC was 6.5 μmol kg^{-1}. The net precipitation during this period resulted in a DIC decrease of 1.2 μmol kg^{-1}. Entrainment of DIC from below the mixed layer decreased the net physical effect to .9 μmol kg^{-1} (13.5%). Biological new production removed 1.1 μmol kg^{-1} (17.5%) of DIC from the mixed layer during the experiment. Air-sea gas exchange had the largest impact on the DIC budget, accounting for 69% (4.5 μmol kg^{-1}) of the total DIC removal from the mixed layer during this period.

5. Estimated Gas Transfer Velocity

The estimated air-sea gas exchange can be used to determine a gas transfer velocity (k) by rearranging the standard flux equation:

$$k = CO_2 \text{ flux} / s\Delta fCO_2 \qquad (4)$$

The CO_2 flux is determined by multiplying the slope of the DIC concentration change by the average mixed layer depth (42 m). The solubility (s) can be estimated from *Weiss* [1974] using the mean mixed layer temperature and salinity. The mean ΔfCO_2 for the experiment was 118±2 μatm based on the shipboard underway pCO_2 measurements [*Wanninkhof et al.*, 2003]. The

estimated mean gas transfer velocity for the period that the GasEx array was in the water was 13.8 cm hr^{-1}. The mean wind speed during this period was 6.0±1.3 m s^{-1}.

Calculating the errors for this estimate should be reasonably straight forward. The three direct estimates that go into these calculations are the slope of the mixed layer DIC change, the mixed layer depth, and the ΔfCO_2. Although measured temperature and salinity values are used to estimate the mean solubility, the errors in these measurements do not make a significant difference to the final number. Propagation of the estimated errors for each of these terms leads to an uncertainty of 3.6 cm hr^{-1} in the final gas transfer velocity. The largest single error in this calculation is in the slope uncertainty. The error estimate used for these calculations was the standard error of the slope. Although some of the inadequacies in the budget accounting are manifested as variability in the daily trends, it is possible that there are systematic biases associated with processes not considered in the budget calculations presented here. At this point, these systematic biases are assumed to be small.

To relate this estimated gas transfer velocity to published results from other approaches, the results presented here must be normalized to a standard Schmidt number (Sc) of 660 according to [*Jähne et al.*, 1987; *Wanninkhof*, 1992]:

$$k_{660} = k_{measured}(Sc_{measured}/660)^{0.5} \quad (5)$$

Based on a local Schmidt number of 482.5 for the study region, the k_{660} from this study is 11.8±3.1 cm hr^{-1} for a mean wind speed of 6±1.3 m s^{-1}. These results agree well with the gas transfer velocity estimates based on eddy correlation measurements made on this cruise [*McGillis et al*., 2003] and are also consistent with the *Wanninkhof* [1992] wind speed formulation (Figure 8).

6. Conclusions

The GasEx-2001 cruise was designed to investigate air-sea gas exchange processes using a variety of different approaches. Many of the air-sea flux techniques used for this study were based on micro-meteorological measurements of atmospheric CO_2 changes with time. The comparable water side changes are relatively large, but are complicated by non-gas exchange processes that can affect the mixed layer DIC concentrations. Budget estimates for mixed layer

DIC during the Lagrangian study period of the GasEx-2001 cruise indicated that, in contrast to previous North Atlantic studies [*Chipman et al.*, 1993; *Feely et al*., 2002], the air-sea gas flux was the largest contributor to the DIC draw-down. A comprehensive suite of measurements and ideal oceanographic conditions also resulted in relatively small error estimates for this study compared to previous studies.

The various estimates and formulations for the gas transfer velocity as a function of wind speed are in reasonable agreement at the mean wind speeds (6 m s^{-1}) observed during the GasEx-2001 experiment (Figure 8). Thus, the mean gas transfer velocity estimated in this study cannot be used to distinguish between the different gas exchange formulations. However, the agreement between the water-side CO_2 loss estimates provided here and the independent atmospheric micro-meteorological CO_2 flux estimates collected on the same cruise supports the validity of the shorter-term approaches for directly evaluating the gas fluxes, which do indicate fluxes that are not consistent with the published relationships [*McGillis et al.,* 2003]. Future gas exchange experiments should continue to include both water-side and air-side flux estimates as independent checks on these approaches.

Acknowledgements. This work was funded by the NOAA Office of Global Programs under the Global Carbon Cycle Program. We thank L. Dilling and D. Rice for supporting the GasEx program. We thank the captain and crew of the *Ronald H. Brown* as well as the scientific party that participated in this cruise. We especially thank D. Greeley, C. Mordy, and D. Hansell for providing the discrete pCO_2, nutrient, and DOC data respectively. R. Wanninkhof and W. McGillis provided helpful comments on early drafts of this manuscript. This publication was partially supported by the Joint Institute for the Study of the Atmosphere and Ocean (JISAO) under NOAA Cooperative Agreement No. NA17RJ11232, JISAO Contribution #956, PMEL contribution #2538.

References

Anderson, L.A. and J.L. Sarmiento, Redfield ratios of remineralization determined by nutrient data analysis, *Global Biogeochem. Cycles*, 8, 65-80, 1994.

Chavez, F.P., and Barber, R.T., An estimate of new production in the equatorial Pacific, *Deep-Sea Res., 34*, 1229-1243, 1987.

Chipman, D. W., J. Marra and T. Takahashi, Primary production at 47°N and 20°W in the North Atlantic Ocean: A comparison between the ^{14}C incubation method and mixed layer carbon budget observations, *Deep-Sea Res. II*, 40, 151-169, 1993.

Chen, H., R. Wanninkhof, R.A. Feely, and D. Greeley, *Measurement of fugacity of carbon dioxide in seawater: An evaluation of a method based on infrared analysis*, NOAA Technical Memorandum ERL AOML-85, 49 pp., 1995.

Coale, K.H., K.S. Johnson, S.E. Fitzwater, R.M. Gordon, S. Tanner, F.P. Chavez, L. Ferioli, C. Sakamoto, P. Rogers, F. Millero, P. Steinberg, P. Nightingale, D. Cooper, W.P. Cochlan, M.R. Landry, J. Constantinou, G. Rollwagen, A. Trasvina, and R. Kudela, A massive phytoplankton bloom induced by an ecosystem-scale iron fertilization experiment in the equatorial Pacific Ocean, *Nature*, 383, 495-501, 1996.

DeGrandpre, M., R. Wanninkhof, W. McGillis, G. Olbu, pCO_2 dynamics in Equatorial Pacific surface waters, *J. Geophys. Res.*, submitted, 2003.

Dickson, A.G., Reference material batch information, http://www-mpl.ucsd.edu/people/adickson/CO2_QC/, 2003.

Dickson A.G., G.C. Anderson and J.D. Afghan, Sea water based reference materials for CO_2 analysis: 1. Preparation, distribution and use. *Mar. Chem*., in press, 2003.

Feely, R.A., R. Wanninkhof, D.A. Hansell, M.F. Lamb, D. Greeley, and K. Lee, Water column CO_2 measurements during the Gas Ex-98 Expedition, In *Gas Transfer at Water Surfaces*, M. Donelan, W. Drennan, E. Saltzman, and R. Wanninkhof (eds.), AGU Geophysical Monograph 127, Washington, D.C., 173-180, 2002.

Gordon, L.I., J.C. Jennings Jr., A.A. Ross and J.M. Krest, A suggested protocol for continuous flow automated analysis of seawater nutrients (phosphate, nitrate, nitrite and silicic acid) in the WOCE Hydrographic program and the Joint Global Ocean Fluxes Study. WOCE Operations Manual, vol. 3: The Observational Programme, Section 3.2: WOCE Hydrographic Programme, Part 3.1.3: WHP Operations and Methods. WHP Office Report WHPO 91-1; WOCE Report No. 68/91. November, 1994, Revision 1, Woods Hole, Mass., USA. 52 loose-leaf pp., 1993.

Gregg, M.C., Estimation and geography of diapycnal mixing in the stratified ocean, in *Physical Processes in Lakes and Oceans, Coastal and Estuarine Studies, Vol. 54*, edited by J. Imberger, 305-338, 1998.

Jähne, B., K.O. Münnich, R. Bösinger, A. Dutzi, W. Huber, and P. Libner, On parameters influencing air-water gas exchange, *J. Geophys. Res*., 92, 1937-1949, 1987.

Johnson, G.C. and M.J. McPhaden, Interior pycnocline flow from the Subtropical to the Equatorial Pacific Ocean, *J. Phys. Oceanogr.*, 29, 3073-3089, 1999.

Johnson, G.C. and C.L. Sabine, Local physical oceanographic conditions during GasEx-2001*, J. Geophys. Res.*, submitted, 2003.

Johnson, G.C., K.E. McTaggart, and J. Hummon, Large scale physical oceanographic context for GasEx-2001*, J. Geophys. Res.*, submitted, 2003.

Johnson, K.M., A.E. King, and J. McN. Seiburth, Coulometric TCO_2 analyses for marine studies; an introduction, *Mar. Chem*., 16, 61–82, 1985.

Johnson, K.M., P.J. leB. Williams, L. Brandstrom, and J. McN. Sieburth, Coulometric total carbon analysis for marine studies: automation and calibration. *Mar. Chem.*, 21, 117–133, 1987.

Liss,P.S., and L. Merlivat, Air-Sea gas exchange rates: Introduction and synthesis, IN The Role of Air-Sea Exchange in Geochemical Cycling, P. Buat-Menard ed., Reidel, Boston, 113-129, 1986.

McGillis, W.R., J.B. Edson, J.E. Hare, C.W. Fairall, Direct covariance air-sea CO_2 fluxes, *J. Geophys. Res*., 106, 16729-16745, 2001a.

McGillis, W.R., J.B. Edson, J.D. Ware, J.W.H. Dacey, J.E. Hare, C.W. Fairall, R. Wanninkhof, Carbon dioxide flux techniques performed during GasEx-98, *Mar. Chem.*, 75, 267-280, 2001b.

McGillis, W., J. Edson, C. Zappa, E. Terray, W. Drennan, M. Donelan, J. Hare, and C. Fairall, Air-sea CO_2 fluxes in the Equatorial Pacific, *J. Geophys. Res., submitted*, 2003.

Strutton P.G., F.P. Chavez, R.C. Dugdale, and V. Hogue, Primary productivity and its impact on the carbon budget of the upper ocean during GasEx-2001, *J. Geophys. Res., submitted*, 2003.

Takahashi, T., J. Olafsson, J.G. Goddard, D.W. Chipman and S.C. Sutherland, Seasonal variation of CO_2 and nutrients in high-latitude surface oceans: A comparative study, *Global Biogeochem. Cycles*, 7, 843-878, 1993.

Tsuchiya, M., Upper waters of the intertropical Pacific Ocean, *Johns Hopkins Oceanogr. Stud.*, 4, 1-50, 1968.

Volk, T. and M.I. Hoffert, Ocean Carbon Pumps: Analysis of the relative strengths and efficiencies in ocean-driven atmospheric CO_2 changes, in *The Carbon Cycle and Atmospheric CO_2: Natural Variations Archean to Present, Geophys. Monogr. Ser.*, vol. 32, edited by E.T. Sundquist and W.S. Broecker, 99-110, AGU, Washington D.C., 1985.

Ward, B., R. Wanninkhof, W.R. McGillis, A.T. Jessup, M.D. Degrandpre, J.E. Hare, and J.B. Edson, Biases in the air-sea flux of CO_2 resulting from ocean surface temperature gradients during GasEx-2001, *J. Geophys. Res., submitted*, 2003.

Wanninkhof, R., Relationship between wind speed and gas exchange over the ocean, *J. Geophys. Res., 97*, 7373-7382, 1992.

Wanninkhof, R. and W. R. McGillis, A cubic relationship between air-sea CO_2 exchange and wind speed, *Geophys. Res. Lett.*, 26 (13), 1889-1892, 1999.

Wanninkhof, R. and K. Thoning, Measurement of fugacity of CO_2 in surface water using continuous and discrete sampling methods, *Mar. Chem.*, 44, 189-204, 1993.

Wanninkhof, R., W. McGillis, and M. DeGrandpre, Gas exchange rates and productivity in the eastern Equatorial Pacific inferred from diurnal changes in surface water pCO_2 and oxygen, *J. Geophys. Res., submitted*, 2003.

Weiss, R.F., Carbon dioxide in water and seawater: the solubility of a non-ideal gas, *Mar. Chem.*, *2*, 203-215, 1974.

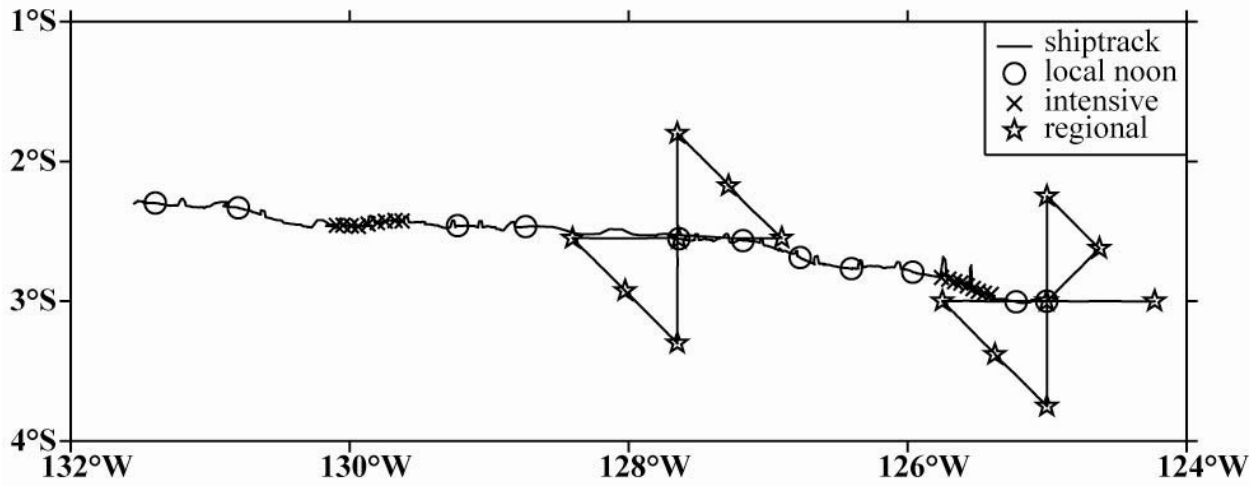

Figure 1. Ship track (solid line) and hydrocast positions during GasEx-2001. Hydrocasts include noon casts near the GasEx array (circles), casts taken near the array during two intensive sampling periods (crosses), and casts collected as part of two regional surveys of the study area (stars). Figure adapted from *Johnson and Sabine* [2003].

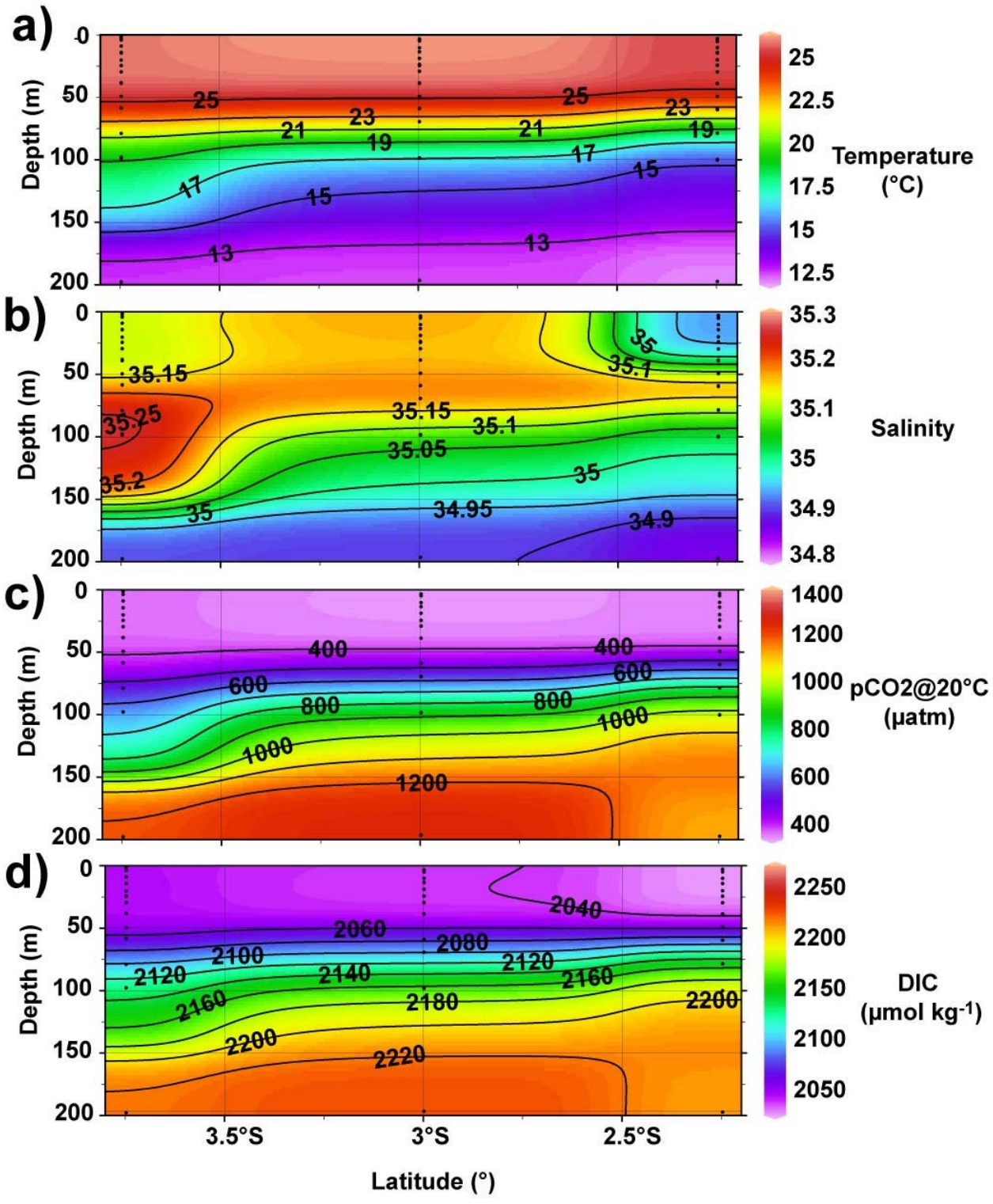

Figure 2. Meridional sections of (a) temperature, (b) salinity, (c) pCO_2 measured at 20°C, and (d) dissolved inorganic carbon from the north-south leg of the first regional survey. Black dots indicate sample locations.

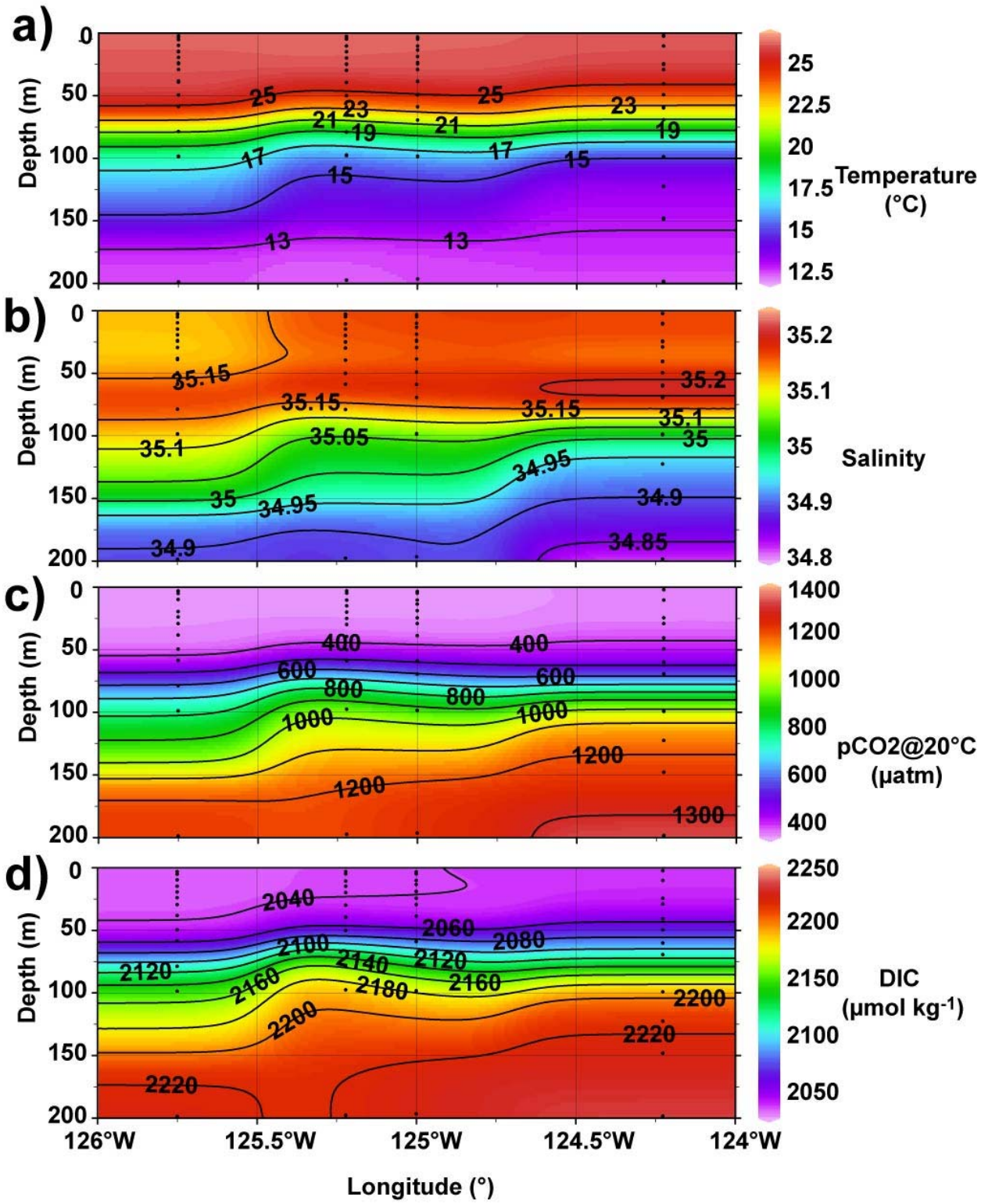

Figure 3. Zonal sections of (a) temperature, (b) salinity, (c) pCO_2 measured at 20°C, and (d) dissolved inorganic carbon from the east-west leg of the first regional survey. Black dots indicate sample locations.

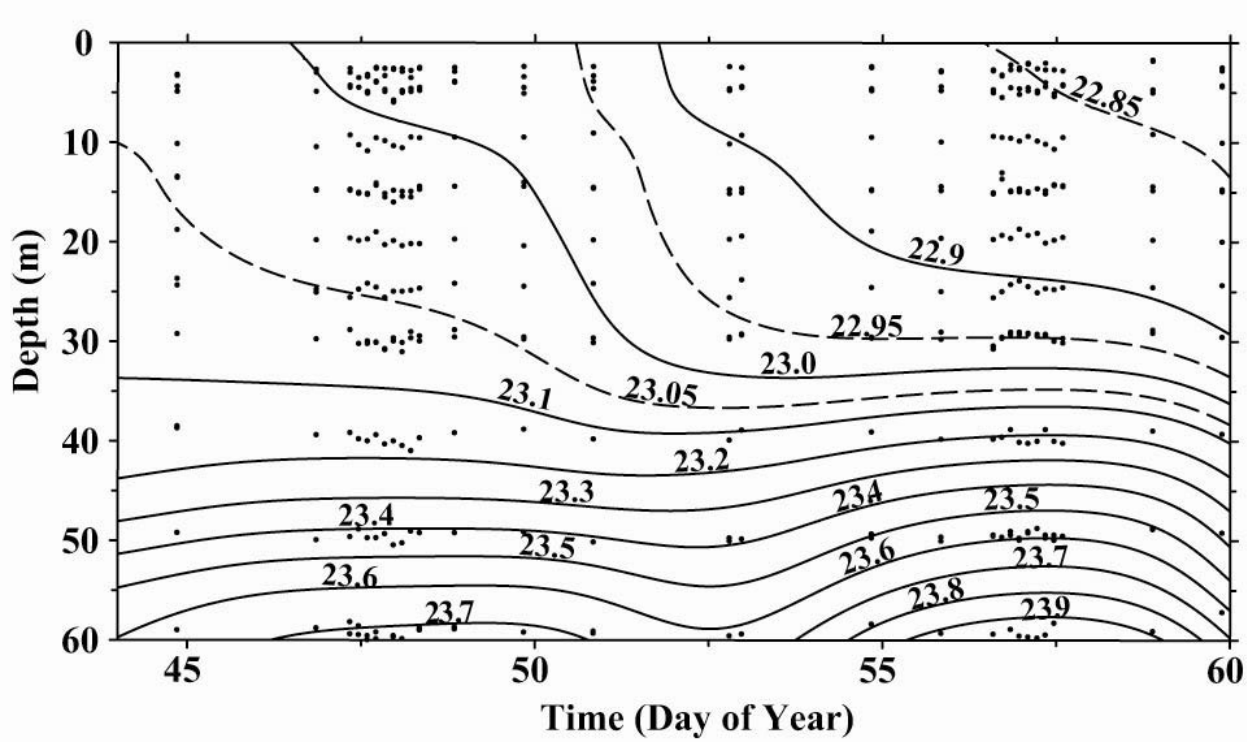

Figure 4. Time-series section of potential density (σ_θ) in the upper 60 m of the water column from casts taken near the GasEx array. Black dots indicate sample locations.

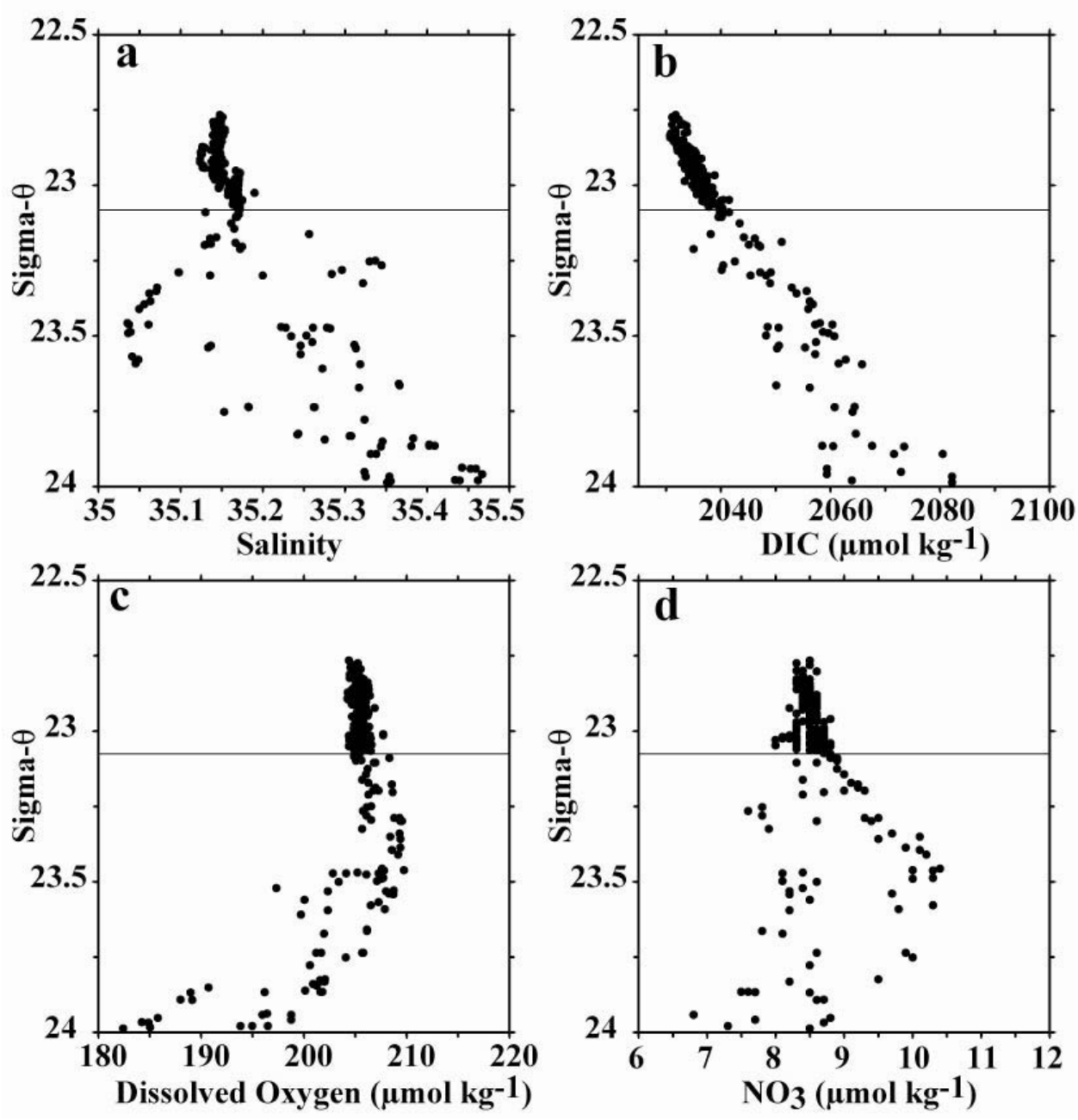

Figure 5. Scatter plots of (a) salinity, (b) dissolved inorganic carbon, (c) dissolved oxygen, and (d) nitrate as a function of potential density. Data are from stations collected near the GasEx array. Horizontal lines indicate the 23.1 kg m^{-3} density surface.

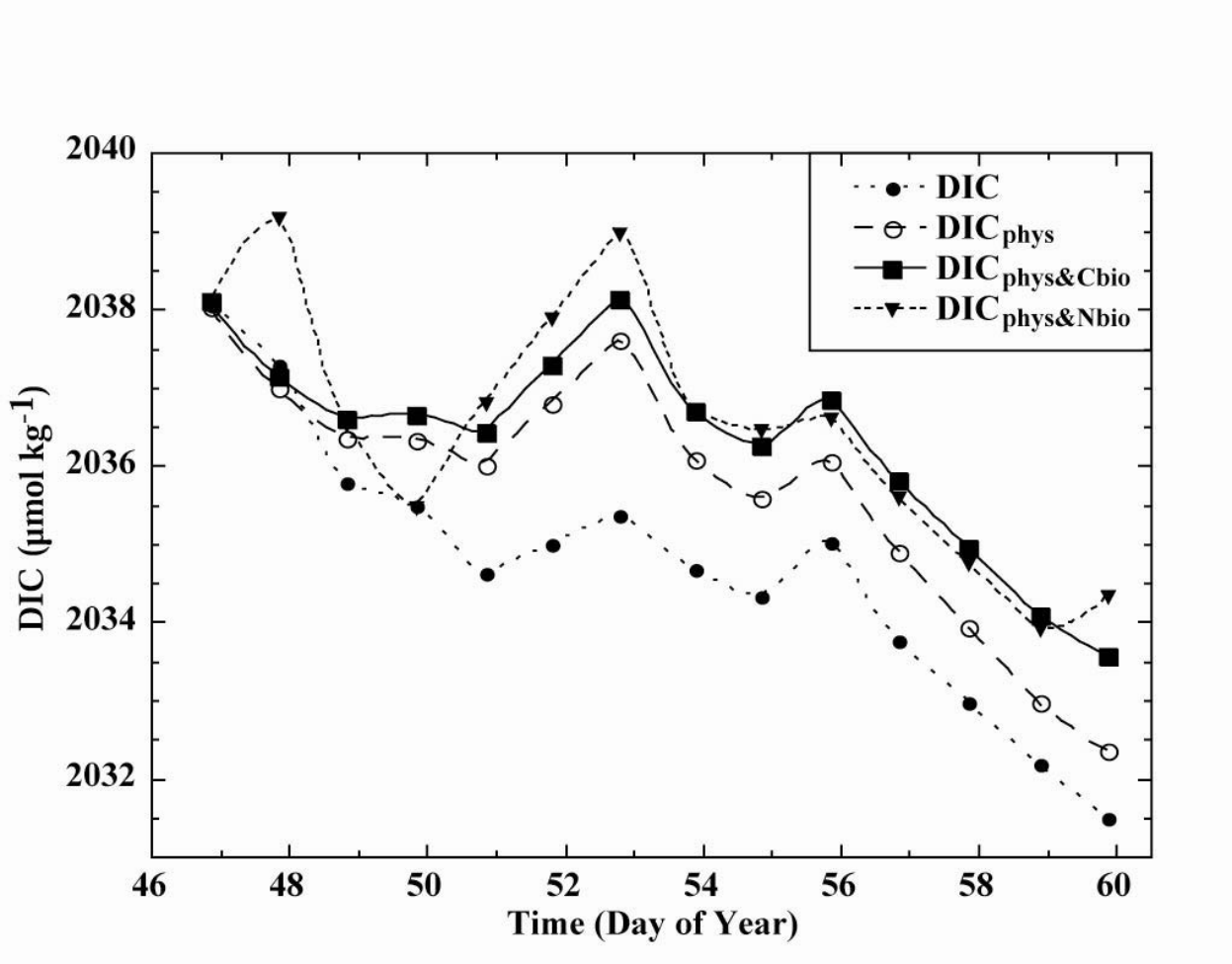

Figure 6. Plot of DIC concentrations as a function of time from the noon casts collected near the GasEx array. Filled circles are the measured DIC concentrations. Open circles are the measured DIC concentrations after the physical fluxes have been removed. The solid squares are the DIC concentrations corrected for the physical fluxes and the biological draw down based on new production estimates. The solid inverted triangles are the DIC concentrations corrected for the physical fluxes and the biological draw down based on changes in dissolved inorganic nitrogen.

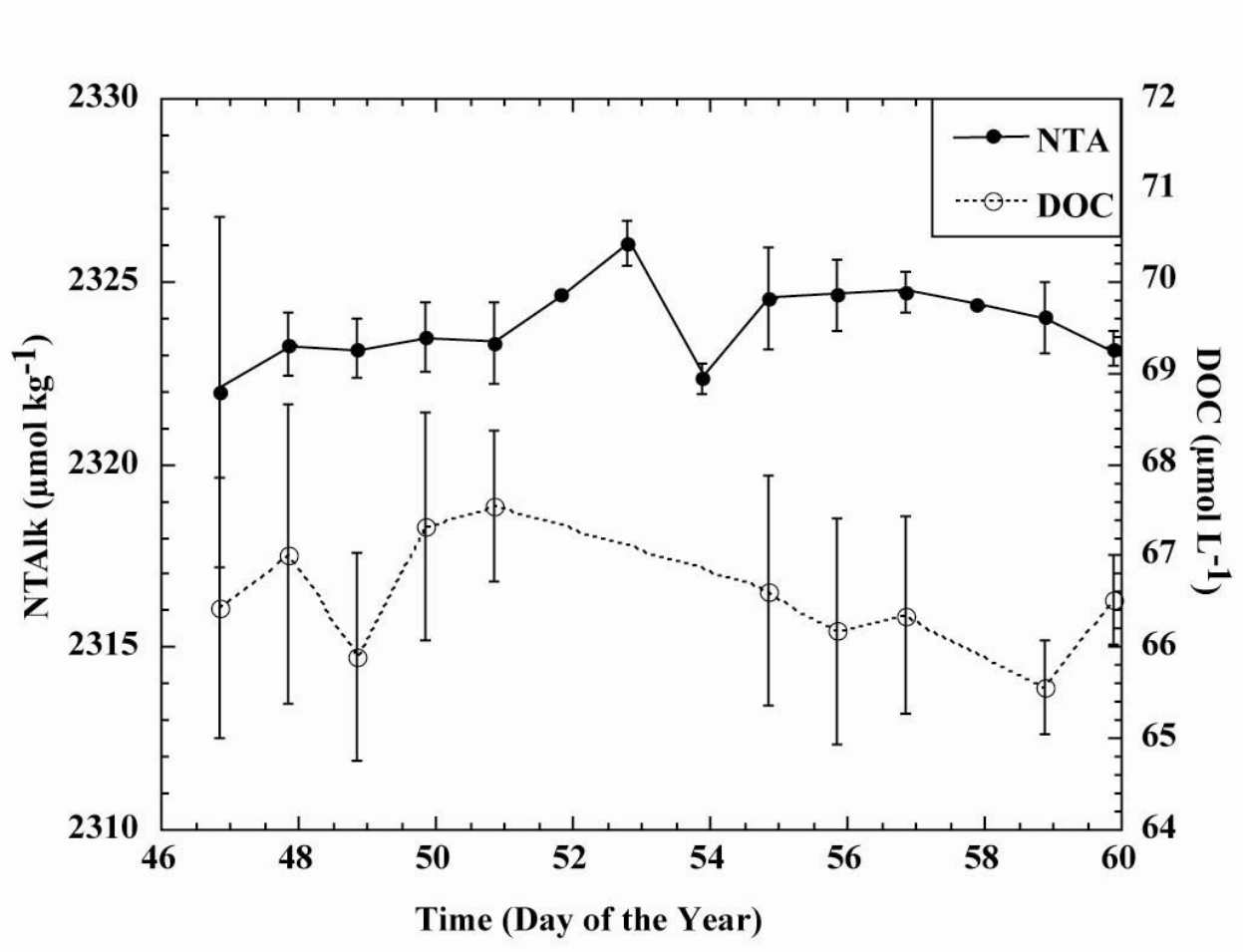

Figure 7. Plot of salinity normalized total alkalinity (filled circles) and dissolved organic carbon (open circles) as a function of time from the noon casts collected near the GasEx array.

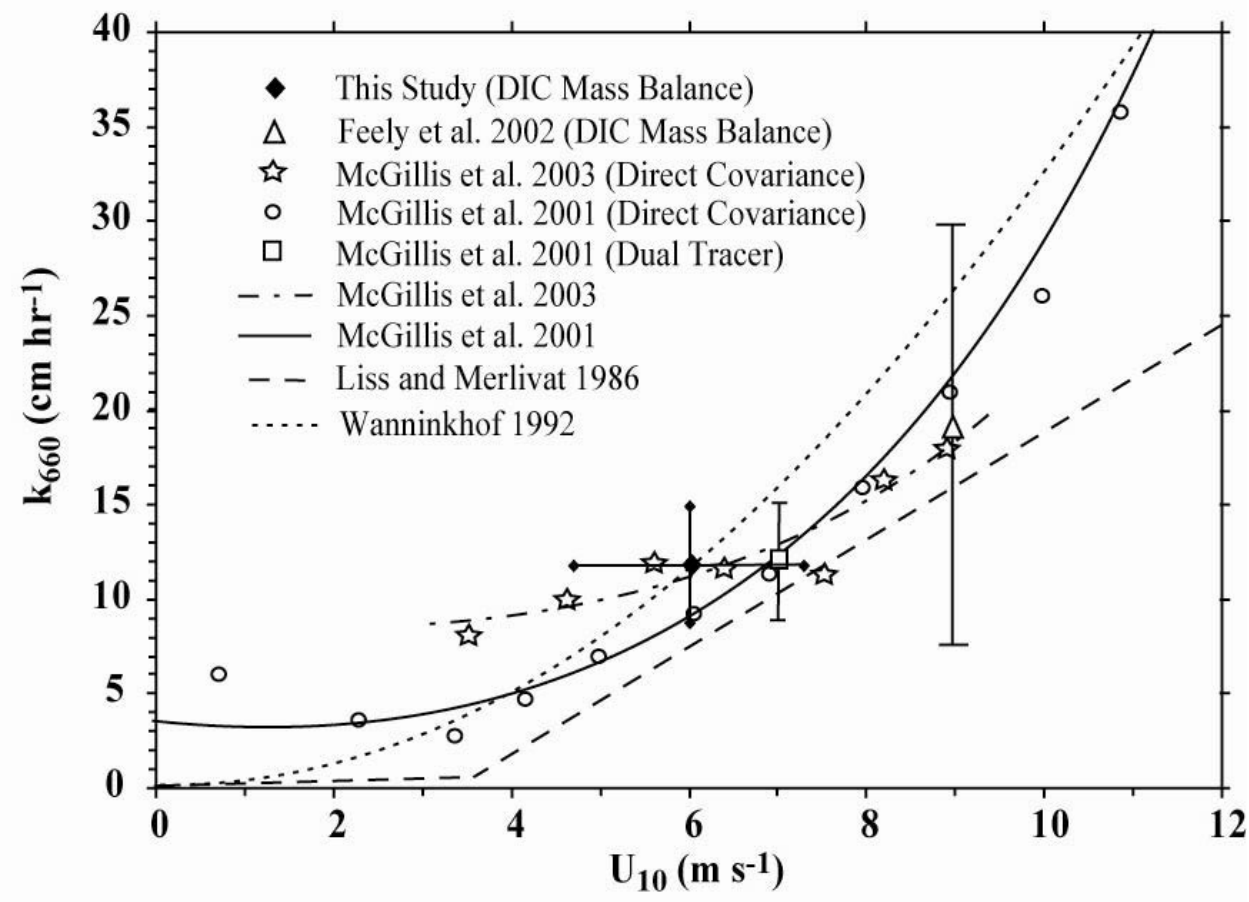

Figure 8. Plot of gas transfer velocity (k_{660}) as a function of windspeed (U_{10}). Dotted line shows *Wanninkhof* [1992] relationship. Solid line shows *McGillis et al.* [2001a] relationship. Dashed line shows *Liss and Merlivat* [1986] relationship. Dash-dot line shows GasEx-2001 relationship from *McGillis et al.* [2003]. Open circles and square with error bars show direct covariance and dual tracer estimates, respectively, from GasEx-98 study [*McGillis et al.*, 2001b]. Stars show direct covariance measurements from GasEx-2001 [*McGillis et al.*, 2003]. Open triangle with error bars shows the estimate from DIC budget on GasEx-98 [*Feely et al*., 2002]. Filled diamond with error bars shows estimate from this study using DIC budget. Figure adapted from *McGillis* [2003].